Applied Catalysis B: Environmental 134–135 (2013) 130–135

Contents lists available at SciVerse ScienceDirect

Applied Catalysis B: Environmental

journal homepage: www.elsevier.com/locate/apcatb

# Air purification by gold catalysts supported on PET nonwoven fabric

Makoto Ikegami[a,b,e], Takanori Matsumoto[a,e], Yuka Kobayashi[a,e], Yohei Jikihara[a,e], Tsuruo Nakayama[a,e,**], Hironori Ohashi[c,e], Tetsuo Honma[d], Takashi Takei[b,e], Masatake Haruta[b,e,*]

[a] NBC Meshtec Inc., 2-50-3 Toyoda, Hino-shi, Tokyo 191-0053, Japan
[b] Graduate School of Urban Environmental Sciences, Tokyo Metropolitan University, 1-1 Minami-osawa, Hachioji, Tokyo 192-0397, Japan
[c] Faculty of Arts and Science, Kyushu University, 744 Motooka, Nishi-ku, Fukuoka 819-0395, Japan
[d] SPring-8/Japan Synchrotron Radiation Research Institute (JASRI), 1-1-1 Kouto, Sayo-cho, Sayo-gun, Hyogo 679-5198, Japan
[e] CREST, Japan Science and Technology Agency (JST), 4-18-8 Hon-cho, Kawaguchi, Saitama 332-0012, Japan

ARTICLE INFO

*Article history:*
Received 8 August 2012
Received in revised form
30 November 2012
Accepted 17 December 2012
Available online 11 January 2013

*Keywords:*
$Au/ZrO_2$ catalyst
PET nonwoven fabric
Gold nanoparticles
Air purification
Formaldehyde
CO

ABSTRACT

A new filter-type $Au/ZrO_2$ catalyst was fabricated by using poly(ethylene terephthalate) (PET) nonwoven fabric as a support. Owing to its flexibility, thinness, lightness, and easy handling, this form of a catalyst is advantageous in practical use for air purification over the existing catalyst forms such as pellets and honeycombs. Zirconium oxide fine particles were first deposited on PET nonwoven fabric in the presence of 3-methacryloxypropyltrimethoxysilane to form thin layer like a fish scale and then gold nanoparticles (NPs) were deposited on $ZrO_2$ fine particles by deposition–precipitation method. The catalyst was active enough at room temperature and oxidized 1000 ppm CO and removed 140 ppm HCHO in air. The catalytic activity of $Au/ZrO_2$ supported on PET nonwoven fabric was also measured under similar conditions to those for practical air purification in offices and houses for the oxidation of 0.5 ppm HCHO and high HCHO conversion (close to 100%) was maintained up to 136 h.



## 1. Introduction

Air circulation in houses, buildings, cars, and trains is being depressed to save energy and in turn the need to indoor air purification has been growing rapidly. In order to solve this dilemma, catalytic removal of odors and hazardous gases at room temperature without using energy for heating appears to be one of the best solutions. In the middle of 1980s one of the present authors reported that gold nanoparticles (NPs) supported on metal oxides exhibited surprisingly high catalytic activity for the oxidative removal of poisonous CO from air [1,2]. Another practical advantage of gold catalysts is that they are activated by moisture [3–5]. These two features distinguish gold catalysts from the conventional catalysts, namely, base metal oxides such as manganese–copper oxides and noble metals such as palladium and platinum. The formers are deactivated by moisture, while the latters are not active enough at room temperature. In 1992 a $Au/Fe_2O_3$ catalyst supported on paper honeycomb together with zeolites was used for the first time as an odor (trimethylamine) eater in modern Japanese toilettes.

The major target gases in current commercial applications are CO and HCHO. Carbon monoxide is a poisonous gas emitted from tobacco smoke, stoves, and fossil fuel burning heaters. There have been fatal accidents by CO poisoning in badly ventilated rooms and kitchens [6]. Formaldehyde is one of the serious sources causing sick building syndrome (SBS). Volatile organic compounds (VOCs) are also emitted from building and furnishing materials. Prolonged exposure to HCHO at concentrations exceeding safe limitations causes serious health problems such as burning sensations in skin, eyes and throat, nausea, difficulty in breathing, and even nasal cancer [7,8]. To prevent significant sensory irritation in our daily life, an air quality guideline value of 0.1 $mg/m^3$ (0.08 ppmv) as a 30 min average is reported for HCHO by the World Health Organization [9].

It has been reported that gold catalysts have high catalytic activity for HCHO oxidation into $CO_2$ and $H_2O$ [10–17]. Generally, catalysts are formed into pellets and beads, or supported on paper, ceramics or metal honeycombs for industrial use, but these forms sometime cause difficulty of handling due to the lack of flexibility. For indoor air purification, active catalysts supported on fabric filter are more convenient owing to its thinness, lightness, and softness. Recently, there are a few studies of gold catalysts supported on fibers for CO oxidation [18,19] and transformation of 4-nitrophenol

* Corresponding author at: Graduate School of Urban Environmental Sciences, Tokyo Metropolitan University, 1-1 Minami-osawa, Hachioji, Tokyo 192-0397, Japan. Tel.: +81 42 677 2852; fax: +81 42 677 2852.
** Corresponding author at: NBC Meshtec Inc., 2-50-3 Toyoda, Hino-shi, Tokyo 191-0053, Japan. Tel.: +81 42 582 2525; Fax: +81 42 582 4440.
*E-mail addresses:* nakayama_t@nbc-jp.com (T. Nakayama), haruta-masatake@center.tmu.ac.jp (M. Haruta).

0926-3373/$ – see front matter © 2013 Elsevier B.V. All rights reserved.
http://dx.doi.org/10.1016/j.apcatb.2012.12.018

to 4-aminophenol [20]. Fang et al. [20] developed gold catalyst supported on electrospun polyethyleneimine/polyvinyl alcohol nanofibers. Kuo et al. [18] developed gold catalysts supported on the glass fiber coated with a layer of $TiO_2$. Koga and Kitaoka [19] developed gold catalysts supported on the paper consisted of ZnO whiskers, ceramic fibers, alumina sol and pulp fibers. Since these methods to support inorganic oxide on fibers need high calcination temperature, the type of fiber materials is limited to heat-resistive one. Moreover, gold NPs deposited on organic polymers did not exhibit catalytic activity in gas phase [21]. Accordingly, there is no report concerning gold catalysts supported on organic polymer for indoor air purification.

In this study, we used radiation graft polymerization technique to homogeneously disperse metal oxide particles on organic fiber surfaces [22] and on inorganic fiber surface [23] without heating. By deposition–precipitation method [24], gold NPs were deposited on $ZrO_2$ which covered the surfaces of PET nonwoven fabric. The fine structure of fabric catalysts were investigated by TEM and XAFS. We first demonstrate here the performance of gold catalysts supported on organic polymer fabric filter for indoor air purification, in particular, CO and HCHO removal.

## 2. Experimental

### 2.1. Preparation of support materials

PET nonwoven fabric coated with $ZrO_2$ fine particles were prepared by a method patented recently [24]. 3-methacryloxypropyltrimethoxysilane (KBM-503, Shin-Etsu Chemical Co., Ltd.) was added into methanol solution under agitation, followed by adjusting pH of the solution to 3 with hydrochloric acid. Then, zirconium dioxide particles (PCS, Nippon Denko Co. Ltd., specific surface area of 31.5 $m^2/g$), (silane coupling agent/$ZrO_2$: 1/20 in weight ratio) were dispersed in the methanol solution by a beads mill. After separating $ZrO_2$ particles modified with silane coupling agent from dispersion by freeze dehydration, the solids were dried at 393 K for 24 h and were dispersed in methanol by a beads mill. Into this dispersion with $ZrO_2$ content of 3 wt%, a PET nonwoven fabric (ELTAS E01040, Asahi Kasei Fibers Corporation, thickness 0.23 mm, weight 40 $g/m^2$) was immersed for 10 s, and then dried for 2 min at 383 K. Subsequently the PET nonwoven fabric was irradiated with 5 Mrad of electron beam for cross-linking at an accelerating voltage of 200 kV.

### 2.2. Deposition of gold NPs

Gold NPs were deposited by the deposition precipitation method [25] on $ZrO_2$ powder or $ZrO_2$ fine particles which covered the surfaces of PET nonwoven fabric. PET non woven fabric covered by $ZrO_2$ ($ZrO_2$/PET), (1.63 g) was immersed in aqueous solution of 5 mmol/L $HAuCl_4$ (100 mL) for different periods (5, 10, 15, and 60 min) at 343 K and to this solution 0.1 mol/L NaOH was added to adjust the pH at 7.0. After deposition precipitation of $Au(OH)_3$, $ZrO_2$/PET was washed with distilled water. After adsorbed water was removed by paper towels, the PET nonwoven fabric was dried in a stream of $N_2$ gas for 4 h at 373 K.

To prepare Au/$ZrO_2$ powder catalysts for reference, the $ZrO_2$ powder (0.5 g) was dispersed in $HAuCl_4$ aqueous solution and treated in a similar manner to $ZrO_2$/PET and then was filtered and washed with distilled water. The residue was dried under reduced pressure for 12 h and then was dried again under the same conditions for PET nonwoven fabric.

### 2.3. Catalytic activity tests

The catalytic activity of the Au/$ZrO_2$ supported on PET nonwoven fabrics (Au/$ZrO_2$/PET) was first measured for the oxidation of 1000 ppm CO. The sample was cut into 2 cm square cubes and 0.3 g of superimposed cut cubes were loaded into a glass reaction tube. A 5 L of Tedlar® sampling bag filled with the reaction gas was connected to the reactor and a total flow rate was controlled at 200 mL/min, which corresponded to a gas hourly space velocity (GHSV) of 8000 $h^{-1}$. The effluent gas from the reactor was gathered into 5 L of Tedlar® sampling bag and analyzed with a gas chromatograph (Agilent Technologies, Inc. GC6890A) equipped with a catalytic methanation converter and a flame ionizaton detector (FID). For comparison, 500 mg of Au/$ZrO_2$ powder was loaded into a glass reaction tube and a total flow rate was adjusted at 300 mL/min with a GHSV of 30,000 $h^{-1}$.

The catalytic CO oxidation and HCHO removal were also performed in a continuous flow fix bed reactor. A reactant gas feed containing 1000 ppm CO in air (with 20 vol% $O_2$) or a gas feed containing 140 ppm HCHO in air (with 20 vol% $O_2$) was passed through the reactor at room temperature and a total flow rate was adjusted at 200 mL/min with a GHSV of 8000 $h^{-1}$. The effluent gas was analyzed with a fourier transform infrared (FTIR) spectrometer (JASCO, FT/IR6100) equipped with a gas cell of 2.5 m optical pathlength and a mercuric cadmium telluride (MCT) detector.

In the catalytic removal of dilute HCHO, the reactant gas (0.5 ppm HCHO, 10 vol% $O_2$, balanced with air) was passed through the reactor with GHSV 8000 $h^{-1}$ at room temperature. The effluent from the reactor was gathered into 5 L of Tedlar® sampling bag at any given point of time-on-stream. Unreacted HCHO in the sampled gas was derivatized by the reaction of 2,4-dinitrophenylhydrazine (DNPH) and its derivative was eluted by acetonitrile and analyzed with a HPLC (Agilent Technologies, Inc. 1120HPLC).

### 2.4. Characterization of the catalysts

The zeta potential of Au/$ZrO_2$/PET and of Au/$ZrO_2$ powder were measured by a zeta potential analyzer (Otsuka Electronics Co.,Ltd ELS-Z2) using electro-osmosis method [26]. The actual loadings of gold and $ZrO_2$ on PET nonwoven fabric and gold on $ZrO_2$ powder were obtained ICP spectroscopy (SII Nano Technology Inc. SPS3520). The chemical states of gold were analyzed by X-ray absorption spectroscopy (XAS). Gold $L_3$-edge XAFS were performed in the transmission mode at the BL14B2 in the SPring-8. The sample specimen was prepared by cutting Au/$ZrO_2$/PET into 1 cm square cubes, and 10 pieces of superimposed sample cubes were sealed in a cell made of polyethylene under ambient atmosphere. X-ray absorption spectra were taken at room temperature. The average diameter of gold was evaluated by observing 310 particles with a transmission electron microscopy (TEM) (JEOL Ltd., JEM-2100F microscope) operating at 200 kV.

## 3. Results and discussion

### 3.1. Deposition of gold NPs on $ZrO_2$ supported by PET nonwoven fabric

Figs. 1 and 2 show the zeta potential and actual gold loading for $ZrO_2$ particles and $ZrO_2$/PET, respectively, as a function of deposition–precipitation time. In the case of deposition–precipitation of $Au(OH)_3$ on $ZrO_2$ particles, deposition started within 1 min. Gold loading reached 0.9 wt% after 10 min and leveled off. The zeta potential decreased rapidly soon after the gold deposition started and, after overshooting, reached a steady

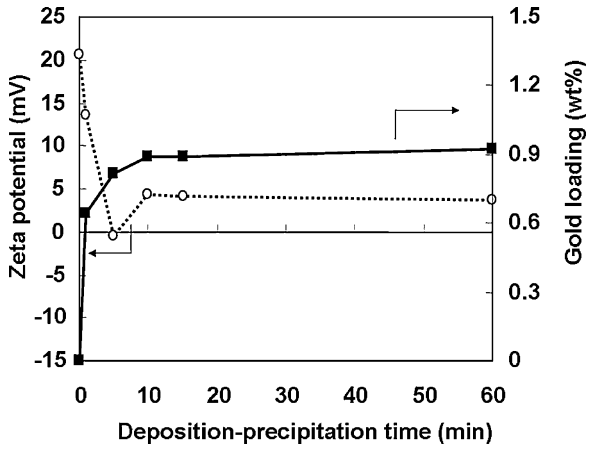


**Fig. 1.** Zeta potential and actual gold loading for $ZrO_2$ particles as a function of deposition–precipitation time.

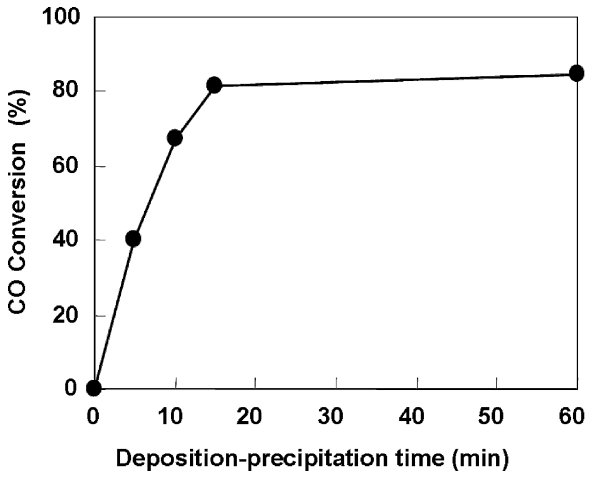


**Fig. 3.** CO conversion at room temperature over $Au/ZrO_2/PET$, as a function of deposition–precipitation time. Loadings to PET: Au 0–1.2 wt%, $ZrO_2$ 7 wt%, reactant gas: 1000 ppm CO, air balance, GHSV: 8000 $h^{-1}$.

state in 10 min. In the case of deposition–precipitation of $Au(OH)_3$ on $ZrO_2$/PET, gold loading increased a little more slowly, probably because of a difference in the interparticle diffusion of gold complex ion into $ZrO_2$ layer, namely, three dimensional diffusion (free $ZrO_2$ powder) and two dimensional diffusion ($ZrO_2$ layer covering the surfaces of PET nonwoven fabric). In both Figs. 1 and 2, zeta potential showed an overshoot toward negative direction, which can be explained by the slow adsorption of cations on the surfaces of $Au(OH)_3$ precipitates.

Fig. 3 shows the influence of deposition–precipitation time on CO conversion over $Au/ZrO_2/PET$. The conversion of CO was almost proportional to an increase in gold loading. Gold deposition on $ZrO_2$/PET is different from that on $ZrO_2$ powder (shown in Figs. 1 and 2). The zeta potential of $ZrO_2$ powder reached a steady state 10 min after deposition of $Au(OH)_3$ started, and gold loading also reached a steady state. It can be assumed that gold deposition is strongly depended on the zeta potential of $ZrO_2$ surfaces, being induced by electrostatic attraction. In the case of $ZrO_2$/PET, it took 15 min until zeta potential reached a steady state. On the other hand, gold loading escalated till 15 min, and increased gradually. It indicates that gold deposition on $ZrO_2$/PET is not only influenced by surface electrical charges but also gold complex ion diffusion near the interface of $ZrO_2$/PET.

### 3.2. Catalytic activity for the oxidation of CO and removal of HCHO

The catalytic activities of the $Au/ZrO_2/PET$ (gold loading 1.5 wt%, and $ZrO_2$ loading 7 wt% to PET) were measured for CO oxidation and HCHO removal in air at room temperature. Fig. 4(a) shows that the oxidation of CO over $Au/ZrO_2/PET$ takes place at room temperature (298 K) with a conversion of 83% after 20 min. However, high catalytic activity and high conversion of CO was gradually decreased with time-on-stream. Konova et al. [28] reported that a gradual decrease in CO conversion was attributed to the formation and accumulation of a monolayer of chemisorbed CO as surface carbonates. These carbonates layer covered the surface of the catalyst and blocked the access of oxygen which was used for CO oxidation. On the other hand, $ZrO_2$/PET without gold NPs did not oxidized CO to $CO_2$ as shown in Fig. 4(b).

Fig. 5 shows HCHO removal efficiency and conversion to $CO_2$ at room temperature over $ZrO_2$/PET. Formaldehyde was not oxidized to $CO_2$ but could be removed by adsorption. HCHO removal efficiency was gradually decreased with time-on-stream toward about 10% adsorption of HCHO. Fig. 6 shows HCHO removal efficiency and conversion to $CO_2$ at room temperature over $Au/ZrO_2/PET$. The removal efficiency of HCHO was maintained

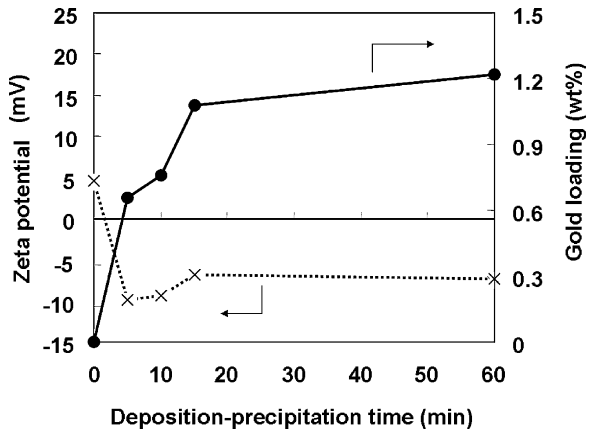


**Fig. 2.** Zeta potential and actual gold loading for $ZrO_2$/PET as a function of deposition–precipitation time.

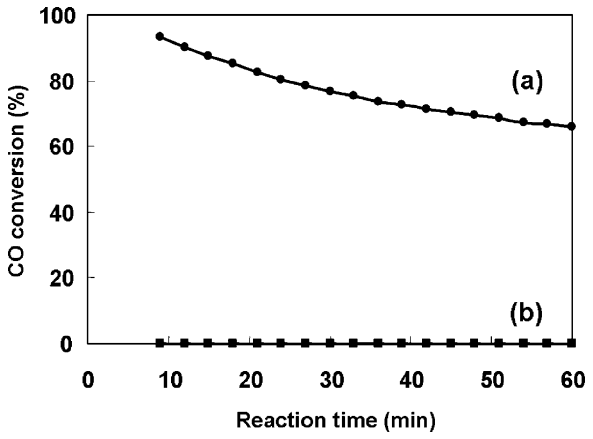


**Fig. 4.** CO conversion at room temperature over (a) $Au/ZrO_2/PET$ and (b) $ZrO_2/PET$ as a function of time-on-stream. Loadings to PET: Au 1.4 wt%, $ZrO_2$ 7 wt%, reactant gas: 1000 ppm CO, air balance, GHSV: 8000 $h^{-1}$.

**Table 1**
Comparison of metal time yield for CO oxidation on A.

| Catalyst samples | Reaction temp. (K) | Metal time yield (mmol g-Au$^{-1}$)[a] | Ref. |
|---|---|---|---|
| 1.5 wt% Au/$ZrO_2$/PET | 298 | $5.5 \times 10^{-2}$ | This study |
| 0.9 wt% Au/$ZrO_2$ (powder) | 298 | $1.4 \times 10^{-2}$ | This study |
| 1.7 wt% Au/$ZrO_2$ (powder) | 298 | $2.0 \times 10^{-3}$ | [29] |
| 0.77 wt% Au/$ZrO_2$ (powder) | 343 | $7.2 \times 10^{-3}$ | [30] |
| 0.01 wt% Au/$ZrO_2$ (powder) | 343 | $2.5 \times 10^{-1}$ | [27] |

[a] The metal time yields (MTYs) were calculated based on the conversions of CO lower than 15%, which were obtained by reducing the contact time in this study. MTYs in the past study made by other groups were calculated based on the conversions of CO lower than 20%, which were obtained at reaction temperature close to 298 K.

**Table 2**
Comparison of MTY for HCHO oxidation on Au/$ZrO_2$/PET and Au/$ZrO_2$ powder.

| Catalyst samples | Reaction temp. (K) | MTY (mmol g-Au$^{-1}$ s$^{-1}$)[a] | Ref. |
|---|---|---|---|
| 1.5 wt% Au/$ZrO_2$/PET | 298 | $1.5 \times 10^{-2}$ | This study |
| 0.9 wt% Au/$ZrO_2$ (powder) | 298 | $5.2 \times 10^{-3}$ | This study |
| 0.85 wt% Au/$ZrO_2$ (powder) | ca. 325 | $6.8 \times 10^{-4}$ | 15 |
| 0.25 wt% Au/$ZrO_2$ (powder) | 333 | $1.7 \times 10^{-1}$ | 16 |

[a] The MTYs were calculated based on the conversions of HCHO lower than 15%, which were obtained by reducing the contact time in this study. MTYs in the past study made by other groups were calculated based on the conversions of HCHO lower than 20%, which were obtained at reaction temperature close to 298 K.

above 90% till 90 min. On the other hand, HCHO conversion to $CO_2$ was gradually increased up to 68% till 36 min and leveled off. Formaldehyde was removed by both adsorption and oxidation to $CO_2$ over Au/$ZrO_2$/PET. The adsorption behavior on $ZrO_2$ alone, Au/$ZrO_2$ and the oxidation behavior on Au/$ZrO_2$ indicates that adsorption is dominant over oxidation till 36 min and then, adsorption reaches equilibrium. These results suggest that HCHO oxidation has two pathways. One is that HCHO is oxidized to $CO_2$ directly over Au/$ZrO_2$ and another is that HCHO is once adsorbed on $ZrO_2$ support and then oxidized to $CO_2$ by Au/$ZrO_2$ catalyst.

Tables 1 and 2 show the comparison of the reaction rate expressed by metal time yield (MTY, conversion of CO or HCHO in mol per unit metal weight per time) for Au/$ZrO_2$/PET and Au/$ZrO_2$ in the oxidation of CO and HCHO and for Au/$ZrO_2$ reported by other groups. Although the catalytic activity per weight of Au/$ZrO_2$/PET was not the highest, Au/$ZrO_2$/PET exhibited the highest MTY for CO oxidation. For HCHO oxidation again, Au/$ZrO_2$/PET exhibited higher catalytic activity than Au/$ZrO_2$ powder, suggesting that Au/$ZrO_2$ grains were more homogeneously dispersed in Au/$ZrO_2$/PET than Au/$ZrO_2$ powder.

In view of air quality guidelines [9], the allowable HCHO concentration is 0.1 mg/m$^3$ (0.08 ppmv) as a 30 min average. The catalytic activity of the Au/$ZrO_2$/PET was measured for the oxidation of HCHO at a concentration of 0.5 ppm. To distinguish catalytic HCHO combustion from HCHO adsorption, $ZrO_2$ supported on PET nonwoven fabric was also tested and the results are shown in Fig. 7. $ZrO_2$/PET without gold NPs could maintain 100% HCHO removal efficiency till 84 h, while HCHO removal efficiency decreased to 55% after 136 h. On the other hand, Au/$ZrO_2$/PET

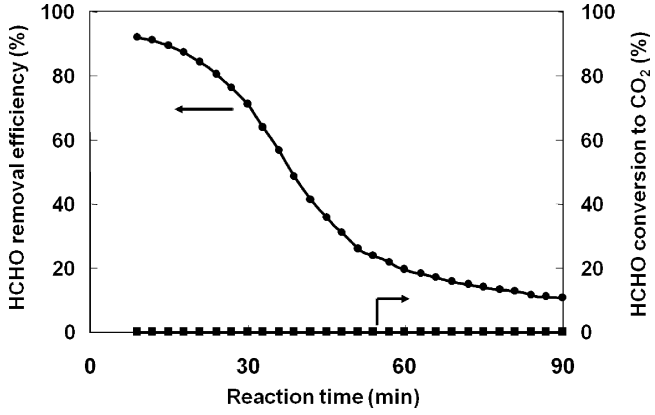


**Fig. 5.** HCHO removal efficiency and conversion to $CO_2$ at room temperature over $ZrO_2$/PET nonwoven fabric, as a function of time-on-stream. Loading to PET: $ZrO_2$ 7 wt%, reactant gas: 140 ppm HCHO, $O_2$ 20 vol%, GHSV: 8000 h$^{-1}$.

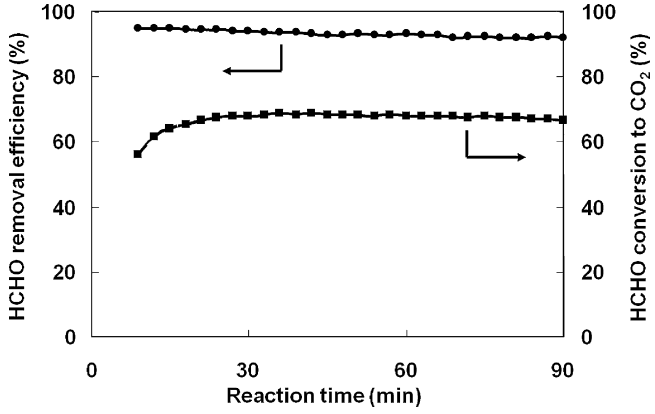


**Fig. 6.** HCHO removal efficiency and conversion to $CO_2$ at room temperature over Au/$ZrO_2$/PET as a function of time-on-stream. Loadings to PET: Au 1.4 wt%, $ZrO_2$ 7 wt%, reactant gas: 140 ppm HCHO, $O_2$ 20 vol%, GHSV: 8000 h$^{-1}$.

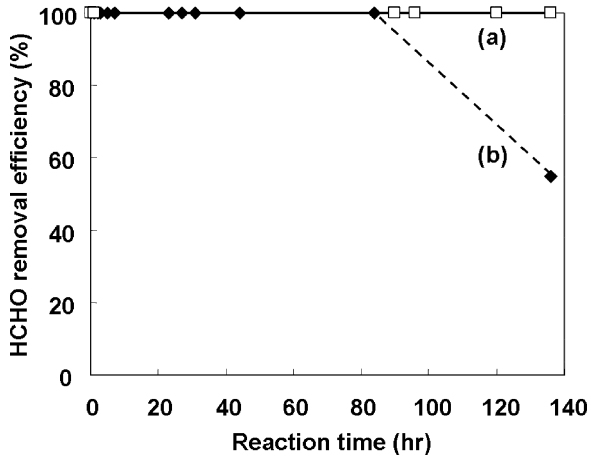


**Fig. 7.** HCHO removal efficiency at room temperature as a function of time-on-stream over (a) Au/$ZrO_2$/PET (□), (b) $ZrO_2$/PET (♦). Loadings to PET: Au 1.4 wt%, $ZrO_2$ 7 wt%, reactant gas: 0.5 ppm HCHO, $O_2$ 10 vol%, air balance, GHSV: 8000 h$^{-1}$.

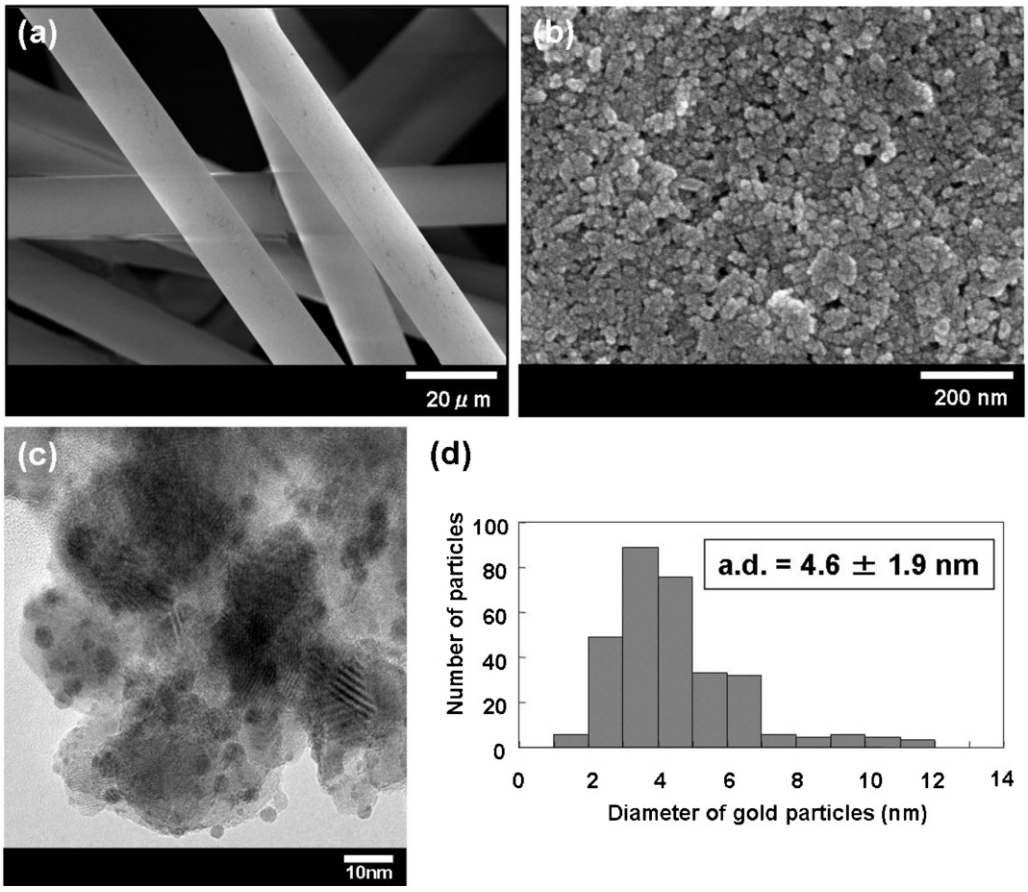


**Fig. 8.** SEM images for (a) PET fibers, (b) fiber surfaces observed with a higher magnification, (c) TEM image of scratched surfaces with high magnification, and (d) the distribution of diameter of gold particles for $Au/ZrO_2$/PET.

maintained 100% HCHO removal efficiency till 136 h and cleared the guideline HCHO value. These results suggest that $Au/ZrO_2$ on PET works efficiently as a catalyst for HCHO oxidation at room temperature.

### 3.3. Characterization of catalysts

$Au/ZrO_2$ catalysts supported on PET nonwoven fabric surfaces were observed by both a SEM and a TEM. SEM photographs for PET fibers and fiber surfaces are shown in Fig. 8(a) and (b). Fine particles of $ZrO_2$ formed a thin film like a fish scale with two-dimensional dispersion to cover the whole surfaces of PET fiber and therefore they did not peel off during gold deposition. Fig. 8(c) shows a TEM photograph for $Au/ZrO_2$ grains covering the outer surfaces of PET fiber. Gold NPs were homogeneously distributed on the whole support surfaces and contacted strongly with $ZrO_2$ fine particles with their flat planes. As shown in Fig. 8(d), the mean diameter of gold particles was estimated to be 4.6 nm from the distribution of the diameters observed for 310 particles. Gold NPs were distributed in a wide size range, however, 70% of them were below 5 nm in diameter. The diameters of gold NPs were similar to those of gold NPs deposited on $ZrO_2$ fine powder, which were previous reported [27,28].

Fig. 9 compares normalized Au-$L_3$ edge XANES spectra for $Au/ZrO_2$/PET together with reference spectra of $Au(OH)_3$ and gold-foil. The $Au/ZrO_2$/PET spectra contained cationic gold species such as $Au(OH)_3$ in addition to metallic gold. It can be interpreted that $Au(OH)_3$ partly remains on $ZrO_2$ particles and/or cationic gold species are present at the perimeter interfaces around metallic gold NPs [21].

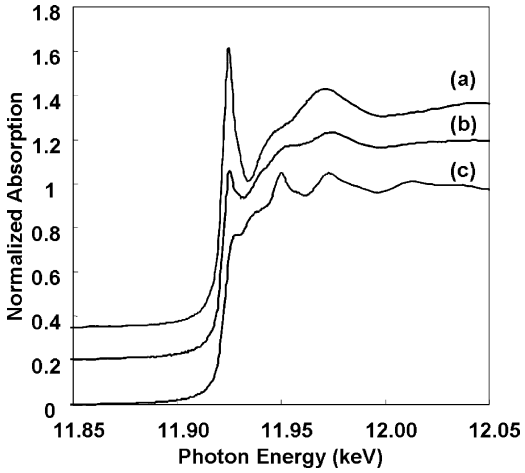


**Fig. 9.** Normalized Au-$L_3$ edge XANES spectra. (a) $Au(OH)_3$ as the reference, (b) $Au/ZrO_2$/PET, and (c) Au-foil as the reference. Loadings to PET: Au 1.5 wt%, $ZrO_2$ 7 wt%.

## 4. Conclusions

A new filter-type gold catalyst has been developed by depositing gold NPs on $ZrO_2$ which was coated on PET nonwoven fabric by graft polymerization technique. This catalytic filter showed good performance in applications to air quality control.

(1) In a stream of 1000 ppm CO in air at an hourly space velocity of 8000 $h^{-1}$ at room temperature, 20 min after the start, the conversion of CO reached 83%. In a stream of 140 ppm HCHO in air at room

temperature, 90% of HCHO was removed with oxidation efficiency to $CO_2$ reaching 68% after 90 min run.

(2) Assuming practical applications to indoor air purification, catalytic activity was measured at a dilute concentration of 0.5 ppm HCHO. It was found that a very high HCHO oxidative removal efficiency close to 100% was obtained for up to 136 h, indicating the practical applicability of the catalytic filter.

## Acknowledgements

This work has been financially supported by JST, CREST.

The synchrotron radiation experiments were performed at the BL14B2 in the SPring-8 with the approval of the JASRI (proposal no. 2009B1007).

## References

[1] M. Haruta, T. Kobayashi, H. Sano, N. Yamada, Chemistry Letters 16 (1987) 405–408.
[2] M. Haruta, Y. Yamada, T. Kobayashi, S. Iijima, Journal of Catalysis 115 (1989) 301–309.
[3] F. Boccuzzi, A. Chiorino, S. Tsubota, M. Haruta, Journal of Physical Chemistry 100 (1996) 3625–3631.
[4] M. Date, M. Haruta, Journal of Catalysis 201 (2001) 221–224.
[5] M. Date, M. Okumura, S. Tsubota, M. Haruta, Angewandte Chemie International Edition 43 (2004) 2129–2132.
[6] J.A. Raub, M. Mathieu-Nolf, N.B. Hampson, S.R. Thom, Toxicology 145 (2000) 1–14.
[7] International Agency for Research on Cancer, IARC Monographs on the Evaluation of the Carcinogenic Risk of Chemicals to Humans, Some Industrial Chemicals and Dyestuffs, Lyon, France, vol. 88, 2006, p. 94.
[8] Agency for Toxic Substance and Disease Registry, Public Health Service, U.S. Department of Health and Human Services, Toxicological Profile for Formaldehyde, NTIS Accession no. PB99-166654, 1999, p. 451.
[9] World Health Organization Regional Office for Europe, in: F. Theakston (Ed.), Air Quality Guidelines for Europe, European Series, No. 91, 2nd ed., WHO Regional Publications, Copenhagen, 2000, p. 87.
[10] M. Haruta, A. Ueda, S. Tsubota, R.M. Torres Sanchez, Catalysis Today 29 (1996) 443–447.
[11] C. Zhang, H. He, Catalysis Today 126 (2007) 345–350.
[12] C. Li, Y. Shen, M. Jia, S. Sheng, M.O. Adebajo, H. Zhu, Catalysis Communications 9 (2008) 355–361.
[13] Y. Shen, X. Yang, Y. Wang, Y. Zhang, H. Zhu, L. Gao, M. Jia, Applied Catalysis B: Environmental 79 (2008) 142–148.
[14] J. Zhang, Y. Jin, C. Li, Y. Shen, L. Han, Z. Hu, X. Di, Z. Liu, Applied Catalysis B: Environmental 91 (2009) 11–20.
[15] Y. Zhang, Y. Shen, X. Yang, S. Sheng, T. Wang, M.F. Adebajo, H. Zhu, Journal of Molecular Catalysis A: Chemical 316 (2010) 100–105.
[16] Y.-C. Hong, K.-Q. Sun, K.-H. Han, G. Liu, B.-Q. Xu, Catalysis Today 158 (2010) 415–422.
[17] C. Ma, D. Wang, W. Xue, B. Dou, H. Wang, Z. Hao, Environmental Science & Technology 45 (2011) 3628–3634.
[18] C.-N. Kuo, H.-F. Chen, J.-N. Lin, B.-Z. Wan, Catalysis Today 122 (2007) 270–276.
[19] H. Koga, T. Kitaoka, SEN'I GAKKAISHI 67 (2011) 47–58.
[20] X. Fang, H. Ma, S. Xiao, M. Shen, R. Guo, X. Cao, X. Shi, Journal of Materials Chemistry 21 (2011) 4493–4501.
[21] M. Haruta, Faraday Discussions 152 (2011) 11–32.
[22] T. Nakayama, N. Motojima, Y. Watanabe, Jpn. Patent 4447354 (2010).
[23] Y. Kobayashi, T. Nakayama, Jpn. Patent, 2010-36500 (2010).
[24] Y. Watanabe, Y. Kobayashi, T. Nakayama, T. Takei, M. Haruta, Jpn. Patent 2010-5568, (2010).
[25] S. Tsubota, M. Haruta, T. Kobayashi, A. Ueda, Y. Nakahara, in: G. Poncelet, P.A. Jacobs, P. Grange, B. Delmon (Eds.), Preparation of Catalysts, vol. V, Elsevier, Amsterdam, 1991, p. 695.
[26] H.-J. Jacobasch, J. Schurz, Progress in Colloid and Polymer Science 77 (1988) 40–48.
[27] X. Zhang, H. Shi, B.-Q. Xu, Catalysis Today 122 (2007) 330–337.
[28] P. Konova, A. Naydenov, T. Tabakova, D. Mehandjiev, Catalysis Communications 5 (2004) 537–542.
[29] J.-D. Grunwaldt, C. Kiener, C. Wogerbauer, A. Baiker, Journal of Catalysis 181 (1999) 223–232.
[30] X. Zhang, H. Wang, B.-Q. Xu, Journal of Physical Chemistry B 109 (2005) 9678–9683.